Electrical Power and Energy Systems 118 (2020) 105764

Contents lists available at ScienceDirect

Electrical Power and Energy Systems

journal homepage: www.elsevier.com/locate/ijepes

Stackelberg game based transactive pricing for optimal demand response in power distribution systems

Changsen Feng[a], Zhiyi Li[b], Mohammad Shahidehpour[c], Fushuan Wen[b,*], Qifeng Li[d]

[a] College of Information Engineering, Zhejiang University of Technology, Hangzhou, Zhejiang 310023, China
[b] School of Electrical Engineering, Zhejiang University, Hangzhou 310027, China
[c] Galvin Center for Electricity Innovation, Illinois Institute of Technology, Chicago, IL 60616 USA
[d] Department of Mechanical Engineering at Massachusetts Institute of Technology, Cambridge, MA 02139, USA

ARTICLE INFO

Keywords:
Bilevel programming
Demand response
Non-cooperative game
Piecewise McCormick relaxation
Transactive price

ABSTRACT

With the implementation of smart distribution technology, the real-time pricing scheme has emerged as a critical subject for energy management systems. In this paper, we propose a bilevel optimization model that computes a transactive price signal representing the impact of wholesale market locational marginal prices on retail customers' demand response participation. At the upper level of the proposed model, the electricity utility company (EUC) determines the optimal energy procurement and transactive price signals for demand response aggregator (DRA). At the lower level, each DRA adjusts its electricity consumption profile using the transactive price signals. The adjusted DRA consumption profile is fed back to the upper level problem as the iteration continues. The interactions among DRAs are simulated as a non-cooperative game. The proposed model is transformed into a mixed-integer quadratically constrained programming through using the Karush-Kuhn-Tucker (KKT) conditions. The generalized disjunctive programming is introduced when linearizing the bilinear terms in KKT conditions by applying piecewise McCormick relaxation and big-M disjunctive constraints. The numerical results demonstrate the effectiveness of our model and the proposed solution method.

1. Introduction

The earlier demand response (DR) programs focused mostly on large consumers [1]. However, the deployment of smart grid and controllable domestic loads allow retail households to participate in DR programs [2]. Several studies analyzed the price-based DR in residential sector through the aggregation of controllable loads which were managed by a DRA [3]. These studies maximized the social welfare through the coordination of energy providers' generation and consumers' electricity demand using day-ahead or real-time pricing. In [4], authors proposed a bilevel model to determine the optimal pricing scheme for DR. In addition, DRAs were simulated as price takers, which reacted to market prices independently in order to reach a competitive equilibrium. Note that the inherent problem in such formulations was the load synchronization when a substantial part of the load was shifted from peak to off-peak hours without reducing peak-to-average ratio significantly [5].

The three-level electricity market hierarchical structure [4], depicted in Fig. 1, is studied in our work. Specifically, we assume the electric utility company (EUC) plays a role of the intermediary agent that bridges the connection between the wholesale market and distribution system aggregators/loads [7]. On the one hand, the EUC determines the optimal bidding strategy based on forecasted electricity prices in a day-ahead wholesale market and energy procurement from variable RESs; on the other hand, the EUC clears the distribution level market by facilitating optimal demand response among end-users. Note that the EUC here not only operates the distribution network, but also plays a dual role of being a retailer with the responsibility of the participation in the wholesale electricity market and readers can refer to [6] and papers therein for more details. As shown in Fig. 1, state-of-the-art distribution management techniques, such as advanced metering infrastructure, facilitate the control of EUC and monitoring of the distribution system. Since a residential consumer has only a few controllable appliances, it is necessary to aggregate the demand response resources from a large number of residential consumers to achieve a sensible benefit to the EUC and consumers. Demands from a heterogeneous population of appliances are aggregated and then dispatched by a DRA. The bidirectional communication between the DRA and the affiliated residents is established using a device referred to as demand controller at the DRA side and using a smart meter at the consumer side [3]. Specifically, the smart meter in each house submits the power

* Corresponding author.
E-mail address: fushuan.wen@gmail.com (F. Wen).

https://doi.org/10.1016/j.ijepes.2019.105764
Received 30 July 2019; Received in revised form 9 November 2019; Accepted 7 December 2019

Nomenclature

A. Acronyms

DER	Distributed energy resources
DR	Demand response
DRA	Demand response aggregator
ESS	Energy storage system
EUC	Electricity utility company
GDP	Generalized disjunctive programming
KKT	Karush-Kuhn-Tucker
MIQCP	Mixed-integer quadratically constrained programming
MPEC	Mathematical programming with equilibrium constraints
RES	Renewable energy source

B. Sets and Indices

$\mathbf{D}$	Set of indices of DR, $\mathbf{D}$: ={1, ...,d, ...,D}
$\mathbf{N}$	Set of buses, $\mathbf{N}$: ={0, 1, ...,n, ...,N}
$\mathbf{T}$	Set of indices of time slots, $\mathbf{T}$: ={1, ...,t, ...,T}
Ω_L	Set of indices of load
Ω_{RES}	Set of indices of renewable generation sources
k	Index of segments in the piece-wise linear utility function

C. Parameters

E_B	Capacity of the ESS(MWh)
E_d^{DR}	Minimal energy consumption of DRA d during the scheduling horizon.
I_i	Phasor of the current injection at bus i, $\mathbf{I} = [I_1, ...I_N]$
$P_{i,t}^L$	Regular load at bus i at time t, $P_{\mathbf{N},t}^L = \sum_{i\in\mathbf{N}} P_{i,t}^L$
$\overline{P}_{i,t}^{RES}$	Available RES power at bus i in time t
$\overline{P}^{ch}/\overline{P}^{dch}$	Maximal charging/discharging rate of ESS
$\overline{P}_{d,t}^{DR}/\underline{P}_{d,t}^{DR}$	Maximum/minimum power consumption of DRA d power at time t
$\mathbf{S}_i$	Complex power injection at bus i, $\mathbf{S} = \mathbf{P} + j\mathbf{Q} = [\mathbf{S}_1, ...,\mathbf{S}_N]$.
$\mathbf{S}_0$	Complex power injection at the slack bus, $S_0 = P_0 + jQ_0$
$\mathbf{V}_0$ /$\mathbf{I}_0$	Voltage/current injection at the slack bus
$\overline{v}_i/\underline{v}_i$	Upper/lower limit on bus voltage magnitude at bus i
V_i	Voltage phasor at bus i, $\mathbf{V} = [V_1, ...,V_N]$
$\Delta\mathbf{V}$	Voltage perturbation vector
$\mathbf{Y}$	The admittance matrix
$\widetilde{\lambda}_t$	Market price forecast in time t
$\Delta\lambda_t$	Deviation of market price from the forecast value at time t
γ_t^R	Retail price for regular load at time t
γ_t^{RES}	Renewable energy price at time t
η^{ch}/η^{dch}	Charging/discharging efficiency of the ESS
ϕ	Capacity of the inverter
$\widetilde{\vartheta}$	Step size of the price signal

D. Variables

$P_{d,t}^{DR}$	Scheduled load for DRA d at time t, $\mathbf{P}_{\mathbf{T},d}^{DR} = [P_{d,1}^{DR}, ...,P_{d,T}^{DR}]$
P_t^0	Power procured from the wholesale market at time t
$P_{i,t}^{RES}/Q_{i,t}^{RES}$	Scheduled active/reactive power of RES at bus i at time t
P_t^{ch}/P_t^{dch}	Charging/discharging power for ESS at time t
SOC_t	State of charge of the ESS at time t
$U_{d,t}$	Utility for DRA d at time t
γ_t^{DR}	Retail price for DRA at time t
λ_t	Uncertain electricity price at the market
ϑ_t	Price signal at time t
α	Lagrangian multipliers
β	Binary variables
ψ	Integer variables for the step of the price signal

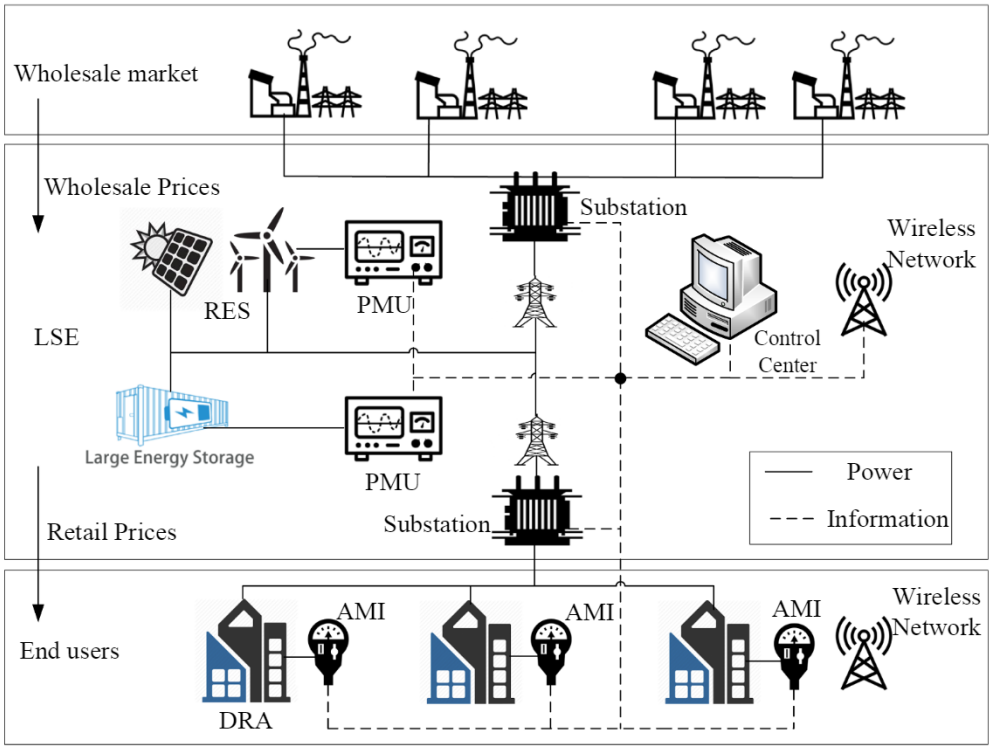

Fig. 1. The conceptual design of the proposed system model.

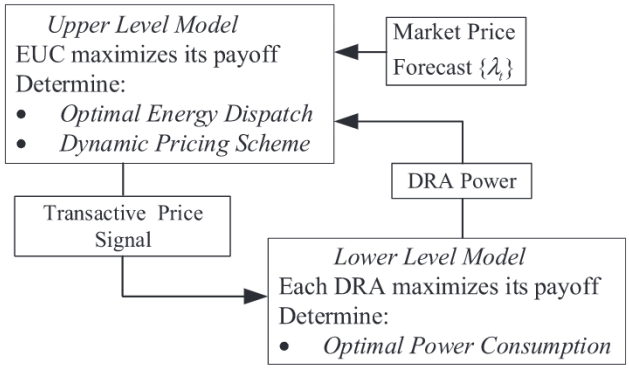

Fig. 2. The proposed bilevel model for transactive pricing.

consumption information, e.g., upper/lower limits of the load power, minimal energy consumption, consumption durations, to the DRA. The DRA is responsible for optimizing the scheduling strategies considering the power consumption information and the price signal published by EUC.

In this paper, we focus our discussion on priced-based DR initiative in order to address the optimal pricing scheme at the retail level. We apply a leader-follower game method in which the hierarchical optimization problem between the EUC and DRAs is modeled as a Stackelberg game with the EUC as the leader (upper problem) and DRAs as followers (lower problems). The proposed model is a bilevel optimization, which represents a special case of mathematical programming with equilibrium constraints (MPEC) [8]. The MPEC model was used in power systems for developing DR dynamic pricing in a distribution network [7], optimal bidding strategy in day-ahead electricity markets [9], optimal pricing strategy in pool-based electricity markets [10], modeling coordinated cyber-physical attacks [11], and optimal charging schedules of plug-in electric vehicles [12].

The MPEC model is conventionally solved by satisfying the KKT conditions or the duality theory [13]. When the Nash equilibrium exists and is unique, the KKT conditions are sufficient and necessary for the optimality of the lower level problem in our model [14]. However, the nonconvexity will result from nonlinear complementarity constraints which could be linearized into Big-M disjunctive constraint through the Fortuny-Amat transformations method [4,7]. Inevitably, a significant number of integer variables were introduced, which resulted in a mix-integer nonconvex model. Besides, the nonlinear complementarity terms were also addressed through semidefinite programming relaxation (SDPR) and reformulation-linearization technique (RLT) [15]. It should be noted that the two methods might incur a large duality gap and a heavy computation time in nonconvex cases. Since the complementarity constraints in KKT conditions comprise many bilinear terms, the piecewise McCormick relaxation [16] was employed to approximate the bilinear terms whereby the model was transformed into a generalized disjunctive programming (GDP) problem with Boolean variables. As the GDP problem could not be solved directly, the convex hull of the disjunctions was introduced [17] to transform the model into a MIQCP problem.

The transactive energy is commonly referred to as a system of economic and control mechanisms that allows the dynamic balance of supply and demand using value as a key operational parameter [18]. A TE framework thus offers a platform for generation and consumption units to automatically negotiate their actions with each other using advanced energy resource management and market algorithms. The existing publications show that the concepts of transactive energy and transactive control are usually applied to subjects like the dispatch of thermostatically controlled loads (e.g. heating, ventilation, and air-conditioning system in commercial buildings) [19], integration of RES into distribution networks [20], and optimal energy management in multi microgrids [21]. In the applications of TE and TC, mechanism design is often one of the most important design factors to ensure their successfulness. Such mechanisms usually aim to set a price signal with incomplete information of players in a market environment so as to induce players to individually make decisions that is optimal to not only themselves but also to global goal maximization (e.g. social welfare). For example, the authors of [22] employ mechanism design to implement the transactive energy management in a local energy market. In addition to mechanism design, the game theory is also widely employed in the framework of TE and TC, which could specifically model strategic interactions among rational decision-makers. The non-cooperative games were widely applied to demand side management where players included microgrids operator [23], distributed generations (DG) and storage devices [24], and household owners [25].

The rest of the paper is organized as follows: Section 2 presents the description of the proposed problem. Section 3 formulates the transactive pricing scheme as a hierarchical optimization problem. Section 4 provides the methodology to transform the model into a tractable MIQCP model. The performance of the proposed model and method is demonstrated in Section 5. Conclusions together with future work are given in Section 6.

2. Problem statement and contributions

In our model, each DRA (i.e., participants in the lower level) determines its power consumption considering the other DRAs' responses as well as the transactive price signals published by the EUC. The DRAs' interactions in the lower problem are simulated by a non-cooperative game in which the Nash equilibrium captures the equilibrium of the transactive energy framework. Thus, the EUC collects power consumption data published by DRAs, and then optimizes the energy procurement and calculates the DRAs' transactive price signal based on the Nash equilibrium of the transactive energy framework. In Fig. 2, a stackelberg game-based payoff maximization model is proposed for EUC which consists of two steps, which is presented as follows.

(1) Upper level – Optimal Energy Dispatch for EUC: EUC calculates the optimal strategy for bidding in the wholesale electricity market which uses DRAs' proposed DR level, uncertain electricity market prices, and energy procurement from variable distributed energy resources (DERs). In this case, EUC minimizes the total cost of purchasing electricity from the bulk market using the worst scenario, which leads to a robust dispatch formulation. In addition, the transactive price signal is calculated by maximizing the social welfare for the bulk locational market price which reduces the DRA's consumption at peak hours and smooths out the EUC's load profile.
(2) Lower level – Transactive Pricing Scheme for DRAs: We constructed a transactive energy framework where DRAs determine their power consumption considering the transactive price signal. More precisely, each DRA is a player in the transactive energy system, which competes with other DRAs by adjusting its power consumption to maximize its payoff function with respect to operation constraints. As we focus on the EUC's day-ahead energy procurement, the EUC optimizes the DRAs' energy procurement and calculates the transactive price signal according to the DRA's power consumption to form the Nash equilibrium.

The contributions of this work are summarized as follows:

1. The proposed approach combines the Stackelberg game with the non-cooperative game when modeling the EUC and DRAs.
2. A new pricing model is proposed which calculates the retail price

considering the total load level to maximize the social welfare.
3. The piecewise McCormick relaxation technique is applied to transform the nonlinear mixed-integer bi-level model into a MIQCP problem.
4. A new method is proposed to linearize the AC power flow equations in order to expedite the solution process.

3. Problem formulation

Before the mathematical formulation is presented, the following assumptions are given:

Assumption 1:. *The EUC and RES producers have a take-or-pay contract. Accordingly, the EUC would purchase all available renewable energy generation from RES suppliers at a fixed price which is normally lower than the electricity price from the main grid.*

Justification: The take-or-pay contract is widely used in European countries and United States [7 26].

Assumption 2:. *The EUC can estimate the price-response characteristics of customers by employing historical price-consumption data.*

Justification: Some papers such as [27] and [28] use mathematical tools, e.g., inverse optimization framework, to simulate the demand-side consumption behavior and further determine the corresponding model parameters for a DRA.

Assumption 3:. *There exists an agreement between the EUC and DRAs to specify an upper limit on the retail price.*

Justification: A large price signal would be unfair for DRAs and a similar assumption is made in [4] and [7].

3.1. Upper level problem

The EUC acquires electricity from the wholesale market and RES producers and sells it to end-users. The EUC aims to maximize its payoff f_L, which is stated as $f_L = Utility - Cost$, where,

$$Utility = \sum_{t\in\mathbf{T}} (\gamma_t^R P_{\mathbf{N},t}^L + \gamma_t^{DR} P_{\mathbf{D},t}^{DR}) \tag{1}$$

$$Cost = \sum_{t\in\mathbf{T}} \left(\lambda_t P_t^0 + \sum_{i\in\Omega_{RES}} \gamma_t^{RES} \overline{P}_{i,t}^{RES}\right) \tag{2}$$

The formulation of DRA's utility is further discussed in Section 3.2. In addition, the EUC's payoff maximization considers the worst-case realization of the wholesale market price, which corresponds to the following robust presentation:

$$\min_{\left\{P_t^0, P_{\mathbf{D},t}^{DR}, \gamma_t^{DR}, P_{i,t}^{RES}\right\}} \max_{\{\lambda_t\in\Omega_\lambda\}} \sum_{t\in\mathbf{T}} \left(\gamma_t^R P_{\mathbf{N},t}^L + \gamma_t^{DR} P_{\mathbf{D},t}^{DR} - \lambda_t P_t^0 - \sum_{i\in\Omega_{RES}} \gamma_t^{RES} \overline{P}_{i,t}^{RES}\right) \tag{3}$$

We define the uncertain set for the wholesale electricity price in a polyhedral representation as:

$$\Omega_\lambda = \left\{ \lambda_t \;\middle|\; \begin{array}{ll} |\lambda_t - \widetilde{\lambda}_t| \leqslant \Delta\lambda_t \;\; \forall\, t\in\mathbf{T} & (\delta_t) \\ \sum_{t\in\mathbf{T}} \frac{|\lambda_t - \widetilde{\lambda}_t|}{\Delta\lambda_t} \leqslant \Gamma & (z_0) \end{array} \right\} \tag{4}$$

The first constraint in (4) ensures that λ_t values are within $[\widetilde{\lambda}_t - \Delta\lambda_t, \widetilde{\lambda}_t + \Delta\lambda_t]$. The second constraint indicates that the total normalized deviation of the market price forecast throughout the scheduling horizon cannot exceed the predefined parameter Γ which is referred as the budget of uncertainty [29]. The budget of uncertainty Γ is within [0, T] which can adjust the robustness of the proposed model. The uncertainty budget can be determined according to a specified confidence level and readers can refer to Appendix. A for details.

As the min-max problem is still intractable for commercial solvers, we introduce an equivalent form and readers can refer to [30–32] for more details. The corresponding robust form of (3) considering the duality theory is stated as

$$\max \sum_{t\in\mathbf{T}} \left(\gamma_t^R P_{\mathbf{N},t}^L + \gamma_t^{DR} P_{\mathbf{D},t}^{DR} - \sum_{i\in\Omega_{RES}} \gamma_t^{RES} \overline{P}_{i,t}^{RES} - \widetilde{\lambda}_t P_t^0 - \delta_t\right) - z_0\Gamma \tag{5}$$

where z_0, δ_t are dual variables and ρ_t is the auxiliary variable and the corresponding feasible set is defined by

$$\begin{cases} -\rho_t \leqslant P_t^0 \leqslant \rho_t, \;\; \delta_t + z_0 \geqslant \Delta\lambda_t \rho_t \\ z_0 \geqslant 0, \; \delta_t \geqslant 0, \; \rho_t \geqslant 0 \end{cases} \forall\, t\in\mathbf{T} \tag{6}$$

The optimization model constraints include power flow equations, bus voltage limits, and operation constraints of inverter-interfaced DERs. A new linearized power flow model is proposed in this paper and we put it in the Appendix. B to make the paragraph more fluent. The limit of voltage magnitude is formulated as:

$$\underline{v}_i \leqslant \|\overline{\mathbf{V}}_i + \Delta\mathbf{V}_i\|_2 \leqslant \bar{v}_i, \;\; \forall\, i\in\mathbf{N} \tag{7}$$

Next, DERs are modeled as RES coupled with an inverter and ESS.

1. RES constraints

For any RES $i \in \Omega_{RES}$ in any time $t \in \mathbf{T}$, we get:

$$\mathbf{S}_i^{RES} \in \mathbf{X}_i^{RES} \tag{8}$$

where $\mathrm{X}_i^{RES} = \left\{ (P_{i,t}^{RES}, Q_{i,t}^{RES}) \,\middle|\, 0 \leqslant P_{i,t}^{RES} \leqslant \overline{P}_{i,t}^{RES}, \; Q_{i,t}^{RES} \leqslant \sqrt{\phi_i^2 - (P_{i,t}^{RES})^2} \right\}$.

2. ESS constraints

It is assumed that the ESS is owned by the EUC and the operation constraints for a single ESS are stated as:

$$\begin{cases} 0 \leqslant P_t^{dch} \leqslant \overline{P}^{dch}, \;\; 0 \leqslant P_t^{ch} \leqslant \overline{P}^{ch} & \forall\, t\in\mathbf{T} \\ SOC_{t+1} = SOC_t + (P_t^{ch}\eta^{ch}/E^B - P_t^{dch}/E^B\eta^{dch}) & \forall\, t\in\mathbf{T}\backslash\{T\} \\ SOC_0 = SOC_T & \\ SOC^{\min} \leqslant SOC_t \leqslant SOC^{\max} & \forall\, t\in\mathbf{T} \end{cases} \tag{9}$$

where SOC_0 denotes the initial state of the ESS. Note that complementarity constraints $P_t^{dch} P_t^{ch} = 0$ can be relaxed [12].

3.2. Lower level problem

At the lower level, DRAs determine their power consumption according to the transactive price signal and other DRAs' responses in a transactive energy framework. The behavior of DRA d is modeled by the concept of utility function $U_{d,t}$ which represents the DRA's satisfaction level stated as a function of its power consumption. Hence, the objective for DRA d is to maximize the payoff function f_d^{DR}, and stated as:

$$f_d^{DR} = \sum_{t\in\mathbf{T}} U_{d,t} - C_d^{DR} \tag{10}$$

where C_d^{DR} is the DRA d purchasing cost from EUC.

It is assumed that the utility function is non-decreasing and concave. Accordingly, a concave quadratic utility function [33] is considered corresponding to a linear decreasing marginal benefit for DRA $d \in \mathbf{D}$ in $t \in \mathbf{T}$, which is stated as:

$$U_{d,t} = \begin{cases} \zeta_{d,t} P_{d,t}^{DR} - \upsilon_{d,t} (P_{d,t}^{DR})^2 & if \;\; 0 \leqslant P_{d,t}^{DR} \leqslant \zeta_{d,t}/2\upsilon_{d,t} \\ (\zeta_{d,t})^2/4\upsilon_{d,t} & if \;\; P_{d,t}^{DR} > \zeta_{d,t}/2\upsilon_{d,t} \end{cases} \tag{11}$$

where $U_d(P_{d,t}^{DR})$ is the DRA's utility function which is approximated by a piecewise-linear function, and stated for DRA $d \in \mathbf{D}$ at $t \in \mathbf{T}$ as

$$U_{d,t} \leqslant a_{d,k,t} P_{d,t}^{DR} + b_{d,k,t} \quad \forall\, k \in \{1, ...,K\} \tag{12}$$

where $a_{d,k,t}$ and $b_{d,k,t}$ are the slope and the intercept of the k-th segment linear utility function for DRA d at time t.

The DRA's payoff function is obtained as

$$f_d^{DR} = \sum\nolimits_{t\in\mathbf{T}} (U_{d,t} - \gamma_t^{DR} P_{d,t}^{DR}) \tag{13}$$

Additionally, we introduce a retail price model for DRA, which is stated as:

$$\gamma_t^{DR} = \varphi(P_{\mathbf{N},t}^{L} + P_{\mathbf{D},t}^{DR}) + \vartheta_t \quad \forall\, t \in \mathbf{T} \tag{14}$$

where φ is the price sensitivity coefficient. The retail price for DRA γ_t^{DR} is composed of two terms. The first term is proportional to the total load level, which can effectively implement the peak-shaving. The second term represents the transactive price obtained from the EUC. In order to mitigate the price volatility, a multi-step piecewise function, as shown in Fig. 3, for the transactive price ϑ_t is employed as:

$$\vartheta_t = \vartheta_{base} + \overline{\vartheta} * \psi_t \tag{15}$$

An upper step limit $|\psi|$ is set for the price ψ_t to alleviate the market power of the EUC. Note that the EUC publishes the transactive price signal ϑ_t, as shown in (15), for DRAs and then DRAs submit their power consumptions the EUC.

For any DRA $d \in \mathbf{D}$ in $t \in \mathbf{T}$, the feasible power region of DRA d, labeled as $\mathbf{X}_d^{DR}$, is formulated as:

$$\mathbf{X}_d^{DR} = \{\underline{P}_{d,t}^{DR} \leqslant P_{d,t}^{DR} \leqslant \overline{P}_{d,t}^{DR} \quad (\alpha_{d,t}^1, \alpha_{d,t}^2)$$

$$U_{d,t} \leqslant a_{d,k,t} P_{d,t}^{DR} + b_{d,k,t} \quad \forall\, k \in \{1, ...,K\} \quad (\alpha_{d,k,t}^3)$$

$$\sum\nolimits_{t\in\mathbf{T}} P_{d,t}^{DR} \geqslant E_d^{DR} \quad (\alpha_d^4)\Big\} \tag{16–18}$$

where $\alpha_{d,t}^1, \alpha_{d,t}^2, \alpha_{d,k,t}^3, \alpha_d^4 \geqslant 0$.

A non-cooperative game is adopted to simulate the transactive market. The EUC clears the transactive market and determine the retail price for the DRA in a Nash equilibrium. Hence, we formulate the following DRA game model:

Players: DRAs in set **D**

Strategies: each DRA $d \in \mathbf{D}$ chooses its power consumption $P_{d,t}^{DR} \in \mathbf{X}_d^{DR}$, to maximize its payoff function.

Payoff function: f_d^{DR} for each DRA $d \in \mathbf{D}$ as stated in (13).

The players' optimal solution is stated as a nonlinear complementarity problem which will be discussed further in Section 4. Accordingly, the proposed bilevel optimization problem is stated as:

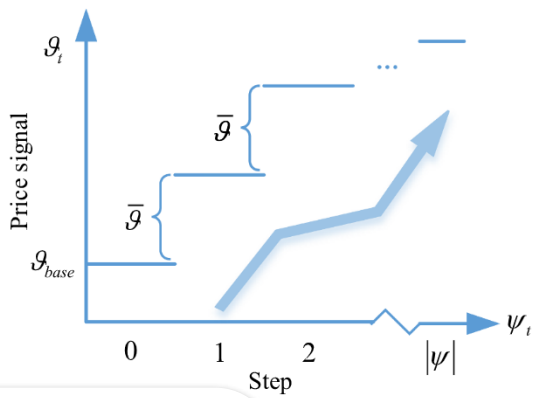

nsactive price.

$$\begin{cases} \textit{The upper level model}\text{: obj.(5), } s.\,t.\ (6)-(9) \\ \textit{The lower level model}\text{: obj.(13), } s.\,t.\ (16)-(18) \end{cases} \tag{19}$$

4. Proposed solution methodology

In this section, we first transform the bilevel optimization problem into a single-level problem. Then, complementarity constraints in the KKT conditions are linearized into a GDP model by a piecewise McCormick relaxation. The rest of bilinear terms are linearized into big-M disjunctive constraints.

4.1. Bilevel to single-level formulation

In this part, we transform the bilevel optimization problem into a single-level problem. The proposed Stackelberg game can be written in a compact form as:

$$\min f_L(x, u_1^*, ...,u_D^*) \tag{20}$$

$$s.\,t. \quad (x, u_1^*, ...,u_D^*) \in \mathbf{X}_L \tag{21}$$

$$u_d^* \in \left\{ \begin{array}{l} \arg\min f_d^{DR}(x^*, u_1, ...,u_D) \\ s.\,t.\ c_d(u_d) \leqslant 0 \quad (\alpha_d) \end{array} \right\} \forall\, d = 1, ...,D \tag{22}$$

where x and u respectively denote the upper and the lower level variables and $\mathbf{X}_L$ represent the feasible region of the upper level variables. The DRA d (the follower) has its own objective f_d^{DR} and constraints c_d of which the Lagrangian multiplier is denoted by α_d. If (20) is convex, the followers choose the optimal strategy using KKT conditions stated as:

$$\begin{cases} \nabla u_d f_d^{DR}(x, u_1, ...,u_D) - \nabla u_d c_d(u_d)\,\alpha_d = 0 \\ 0 \leqslant \alpha_d \perp c_d(u_d) \leqslant 0 \end{cases} \forall\, d = 1, ...,D \tag{23}$$

where $\alpha_d \perp c_d(u_d) \Leftrightarrow \alpha_d * c_d(u_d) = 0$.

If the lower level problem (20) is a non-cooperative game with a unique Nash equilibrium, the model (20)–(22) is an MPEC problem. Thus, we transform the MPEC problem into single-level as follows:

$$\begin{cases} \min f_L(x, u_1, ...,u_d) \\ s.\,t.\ \{(21), (23)\} \end{cases} \tag{24}$$

Here we define $\mathbf{P}_{\mathbf{T},\mathbf{D}}^{DR} = [P_{\mathbf{T},1}^{DR}, ...,P_{\mathbf{T},D}^{DR}]'$. The Nash equilibrium is stated as $\mathbf{P}_{\mathbf{T},\mathbf{D}}^{DR(*)}$ for any $d \in \mathbf{D}$,

$$f_d^{DR}(\mathbf{P}_{\mathbf{T},d}^{DR(*)}, \mathbf{P}_{\mathbf{T},-d}^{DR}) \geqslant f_d^{DR}(\mathbf{P}_{\mathbf{T},d}^{DR}, \mathbf{P}_{\mathbf{T},-d}^{DR})\ \forall\, \mathbf{P}_{\mathbf{T},d}^{DR} \in \mathrm{X}_d^{DR} \tag{25}$$

where $\mathbf{P}_{\mathbf{T},-d}^{DR}$ denotes the total DRAs' power consumption excluding DRA d, i.e., $\mathbf{P}_{\mathbf{T},-d}^{DR} = \{\mathbf{P}_{\mathbf{T},1}^{DR}, ...,\mathbf{P}_{\mathbf{T},d-1}^{DR}, \mathbf{P}_{\mathbf{T},d+1}^{DR}, ...,\mathbf{P}_{\mathbf{T},D}^{DR}\}$. As the payoff function, shown in (13), is concave and continuous, and the decision variable for each DRA, e.g. $P_{d,t}^{DR}$, is assumed continuous, we offer the following theorem:

Theorem:. *The Nash equilibrium at the lower level model always exists and is unique.*

Proof:. *Please see Appendix. C.*

Thus, for any DRA $d \in \mathbf{D}$ in $t \in \mathbf{T}$, the KKT conditions for the lower level problem are stated as:

$$\varphi(P_{d,t}^{DR} + P_{\mathbf{N},t}^{L} + P_{\mathbf{D},t}^{DR}) + \vartheta_t + \alpha_{d,t}^1 - \alpha_{d,t}^2 - \sum\nolimits_k a_{d,k,t}\alpha_{d,k,t}^3 - \alpha_d^4 = 0 \tag{26}$$

$$\sum\nolimits_{k=1}^{K} \alpha_{d,k,t}^3 = 1 \tag{27}$$

$$0 \leqslant \overline{P}_{d,t}^{DR} - P_{d,t}^{DR} \perp \alpha_{d,t}^1 \geqslant 0 \tag{28}$$

$$0 \leqslant P_{d,t}^{DR} - \underline{P}_{d,t}^{DR} \perp \alpha_{d,t}^2 \geqslant 0 \tag{29}$$

$$0 \leqslant b_{d,k,t} + a_{d,k,t} P_{d,t}^{DR} - U_{d,t}^{DR} \perp \alpha_{d,k,t}^3 \geqslant 0 \quad \forall\, k = 1, ...,K \tag{30}$$

$$0 \leqslant -E_d^{DR} + \sum_{t\in\mathbf{T}} P_{d,t}^{DR} \perp \alpha_d^4 \geqslant 0 \tag{31}$$

4.2. Piecewise McCormick relaxation

Here, we apply the piecewise McCormick relaxation and represent the relaxed model as a GDP problem. As the GDP problem cannot be directly solved, we derive a convex hull to relax the problem into a convex model.

First, if $w_{ij} = x_i x_j$, the McCormick relaxation is written as:

$$\begin{cases} w_{ij} \geqslant x_i^l x_j + x_j^l x_i - x_i^l x_j^l, \;\; w_{ij} \geqslant x_i^u x_j + x_j^u x_i - x_i^u x_j^u \\ w_{ij} \leqslant x_i^l x_j + x_j^u x_i - x_i^l x_j^u, \;\; w_{ij} \leqslant x_i^u x_j + x_j^l x_i - x_i^u x_j^l \end{cases} \tag{32}$$

where $x_i^l \leqslant x_i \leqslant x_i^u$, $x_j^l \leqslant x_j \leqslant x_j^u$.

For clarity, (26)–(30) are written in a compact form as $\mathbf{g}(P_{d,t}^{DR}, \alpha) \leqslant 0$. If $\mathbf{w}$ denotes the bilinear terms in $\mathbf{g}(P_{d,t}^{DR}, \alpha)$, $\mathbf{g}(P_{d,t}^{DR}, \alpha, \mathbf{w}) \leqslant 0$ represents the same set as $\mathbf{g}(P_{d,t}^{DR}, \alpha) \leqslant 0$ where the corresponding bilinear terms are relaxed in the McCormick relaxation form.

Assuming that $P_{d,t}^{DR}$ is partitioned into L segments, $\underline{P}_{d,t}^{DR(\ell)}$ and $\overline{P}_{d,t}^{DR(\ell)}$ denote lower and the upper bounds of $P_{d,t}^{DR}$ for partition ℓ, respectively. For $t \in \mathbf{T}$, constraints (26)–(30) are written in the GDP form as:

$$\bigvee_{\ell \in \{1,2,\ldots,L\}} \begin{bmatrix} \mathrm{Y}_\ell \\ \underline{P}_{d,t}^{DR(\ell)} \leqslant P_{d,t}^{DR} \leqslant \overline{P}_{d,t}^{DR(\ell)} \\ \mathbf{g}(P_{d,t}^{DR}, \alpha, \mathbf{w}) \leqslant 0 \end{bmatrix} \tag{33}$$

where the Boolean variable $\mathrm{Y}_\ell \in \{True, \; Flase\}$. Note that in the disjunctions only one of the Boolean variables Y_ℓ is true.

Introducing auxiliary variables τ, we describe the convex hull of disjunctions in (33) [17].

$$\begin{cases} \tau^{(\ell)} \underline{P}_{d,t}^{DR(\ell)} \leqslant P_{d,t}^{DR(\ell)} \leqslant \tau^{(\ell)} \overline{P}_{d,t}^{DR(\ell)} \\ \tau^{(\ell)} \mathbf{g}(P_{d,t}^{DR(\ell)}/\tau^{(\ell)}, \alpha^{(\ell)}/\tau^{(\ell)}, \mathbf{w}^{(\ell)}/\tau^{(\ell)}) \leqslant 0 \\ 0 \leqslant \tau^{(\ell)} \leqslant 1 \qquad\qquad \forall \ell \in \{1, \ldots, L\} \\ \sum_{\ell=1}^{L} \tau^{(\ell)} = 1 \\ P_{d,t}^{DR} = \sum_{\ell=1}^{L} P_{d,t}^{DR(\ell)} \end{cases} \tag{34}$$

We give an intuitive example to demonstrate the importance of convex hull for improving the relaxation performance. Consider the bilinear terms $xy = 1$ and $0.5 \leqslant x \leqslant 2$, $0.5 \leqslant y \leqslant 2$. In Fig. 4, the orange line denotes the linear constraints, i.e., (26)-(27). If we directly apply the McCormick relaxation, the relaxed region will be the union of red and blue areas. However, when employing the piecewise McCormick relaxation, the corresponding convex hull obtained from (33) shrinks to the red area. Thus, the proposed relaxation in our method is tighter and thus guarantees a more accurate solution.

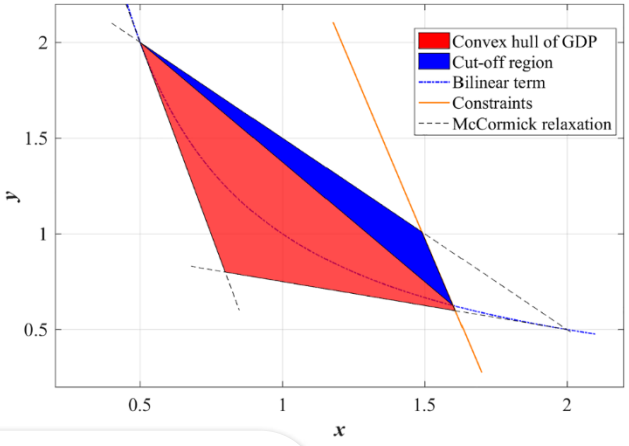

the GDP convex hull.

4.3. Fortuny-Amat transformations method

As (31) is temporally coupled with T bilinear terms for any $d \in \mathbf{D}$, it is unreasonable to directly apply the McCormick relaxation as it may incur a large gap and many constraints. Accordingly, (31) is relaxed into big-M disjunctive constraints based on the Fortuny-Amat transformation, which introduces $\mathbf{D}$ integer variables and may not increase the computational burden. Hence, for any $d \in \mathbf{D}$, (31) is be reformulated as:

$$\begin{cases} 0 \leqslant \sum_{t\in\mathbf{T}} P_{d,t}^{DR} - E_d^{DR} \leqslant M\beta_d^1 \\ 0 \leqslant \alpha_d^4 \leqslant M(1-\beta_d^1) \end{cases} \tag{35}$$

where $\beta_d^1 \in \{0, 1\}$ and M is a big number. An analytical approach is provided in Appendix. D to determine the minimum value of M.

There are still some bilinear terms in the objective functions. Similarly, $\widetilde{\mathfrak{d}}\psi_t P_{\mathbf{D},t}^{DR}$ is transformed into bilinear expressions by a binary expansion described as:

$$\begin{cases} \widetilde{\mathfrak{d}}\psi_t P_{\mathbf{D},t}^{DR} = \widetilde{\mathfrak{d}}(2^0\beta_{t,0}^2 P_{\mathbf{D},t}^{DR} + 2^1\beta_{t,1}^2 P_{\mathbf{D},t}^{DR} + \ldots + 2^{\bar{\nu}}\beta_{t,\bar{\nu}}^2 P_{\mathbf{D},t}^{DR}) \\ \qquad 0 \leqslant 2^0\beta_{t,0}^2 + 2^1\beta_{t,1}^2 + \ldots + 2^{\bar{\nu}}\beta_{t,\bar{\nu}}^2 \leqslant |\psi| \end{cases} \tag{36}$$

where $\beta_t^2 \in \{0, 1\}$. For given a real number a, $\lfloor a \rfloor$ rounds a to the nearest integer towards minus infinity. The integer $\bar{\nu}$ is determined by $\bar{\nu} = \lfloor \log_2(|\psi|) \rfloor$. For any $\nu \leqslant \bar{\nu}$ in any time slot $\forall\, t \in \mathbf{T}$, the bilinear terms in (36) are linearized as:

$$\begin{cases} P_{\mathbf{D},t}^{DR} - M(1-\beta_{t,\nu}^2) \leqslant \theta_{t,\nu} \leqslant P_{\mathbf{D},t}^{DR} + M(1-\beta_{t,\nu}^2) \\ \qquad -M\beta_{t,\nu}^2 \leqslant \theta_{t,\nu} \leqslant M\beta_{t,\nu}^2 \end{cases} \quad \forall\, \nu = 0, 1, \ldots, \bar{\nu} \tag{37}$$

where $\theta_{t,\nu} = P_{\mathbf{D},t}^{DR}\beta_{t,\nu}^2$. Here the minimum value of M can be set as $\overline{P}_{\mathbf{D},t}^{DR}$.

Accordingly, the original model is transformed into a MIQCP problem which is stated as:

$$\begin{cases} \text{obj.(5)} \\ s.\,t.\ (6)-(9),\ (34)-(35),\ (37) \end{cases} \tag{38}$$

5. Numerical results

In this section, we consider the modified IEEE 33-bus and 123-bus test systems to demonstrate the performance of our model. The numerical experiments are conducted in MATLAB R2014a on a personal computer with an Intel Core (i7, 2.80 GHz) and 8 GB memory. SCIP 3.2 is invoked to solve the MIQCP.

5.1. Simulation data

We assume the EUC owns an ESS, located at the slack bus, and does not own any RES. The EUC has take-or-pay contracts with local RES farms for fixed price purchases. Given that the photovoltaic (PV) arrays represent a dominant DG in medium and low voltage distribution systems, we only apply PVs to our test cases with the corresponding data given in [34]. We assume all the PV arrays share the same solar irradiance. The ESS parameters are given in Table 1.

The electricity price forecasts and load variances are taken from the PJM website [35]. A time-of-use (TOU) scheme is also considered,

Table 1
ESS parameter values.

$\overline{P}^{dch}$(MW)	$\overline{P}^{ch}$(MW)	E_B(MWh)	$SOC^{\max}$	$SOC^{\min}$	η^{ch}	η^{dch}
0.6	0.6	3	0.95	0.1	0.9	0.9

Table 2
System parameters.

Parameter	Value	Parameter	Value
γ^R	50$/MWh	φ	38$/MWh
γ^{RES}	30$/MWh	ϑ_{base}	20$/MWh
$\bar{P}^{DR}$	0.8 MW	P^{DR}	0.16 MW
E^{DR}	11.60MWh	$\bar{\varpi}$	14 $/MWh
υ	1100	ζ	630
Γ	8	$\Delta\lambda$	$0.1\tilde{\lambda}$
K	3		

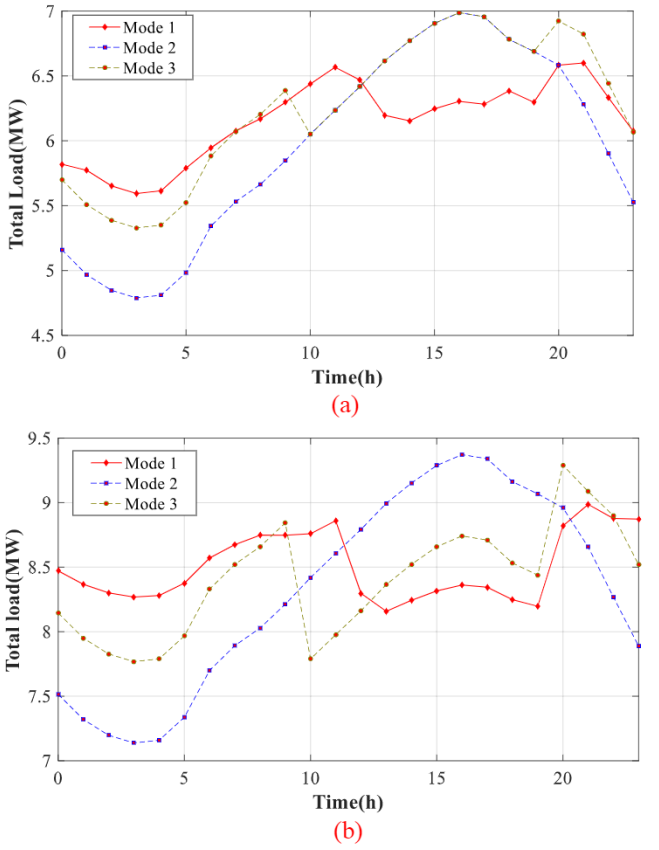

Fig. 5. Total power consumption in modes 1, 2 and 3: (a) IEEE 33-bus test system, (b) IEEE 123-bus test system.

which divides a single day into peak and off-peak hours. We assume 3 DRAs connected at buses 17, 20, 32 in the 33-bus test system, and 7 DRAs at buses 13, 23, 44, 54, 72, 108, 116 in the 123-bus system, use the same parameters. The DRA power factor is 0.89. The system parameters and DRA data are given in Table 2 with the additional data presented in [36].

5.2. Performance of modes

- **Mode 1**: Consider the proposed optimization model. DRAs choose an optimal solution according to EUC's price signals.
- **Mode 2**: Consider the fixed retail price applied to DRAs. In this mode, DRAs have no incentives to adjust their loads.
- **Mode 3**: Consider TOU pricing for DRAs.

To demonstrate the effectiveness of our model, we assume there is no ESS integrated into the network in three modes; we will study the

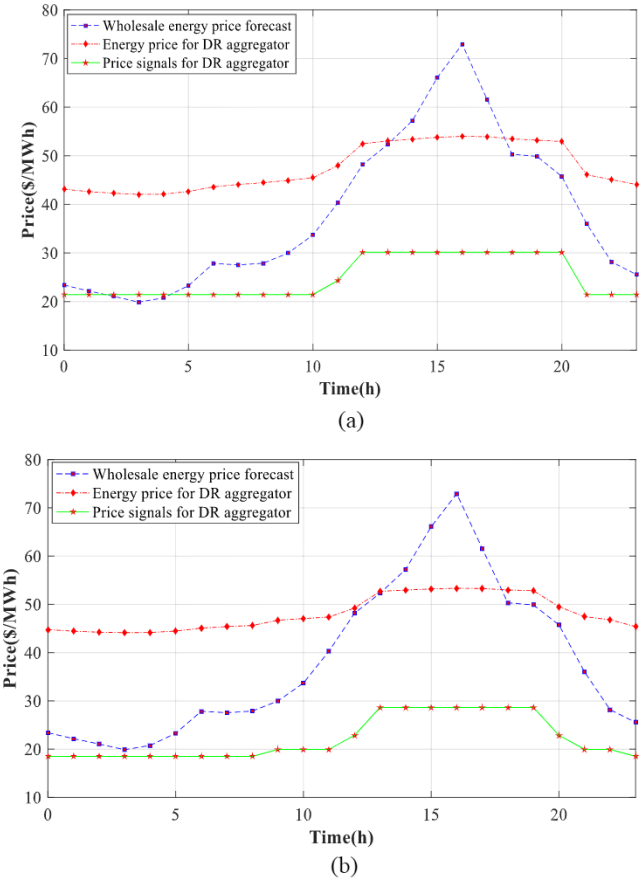

Fig. 6. Price for DRA: (a) 33-bus test system, (b) 123-bus test system.

Table 3
Comparisons between three modes for 33-bus system.

	Mode 1	Mode 2	Mode 3
EUC's payoff ($)	1242.3	1174.3	1255.1
DRA payment ($)	1867.2	2071.3	2152.2
DRA consumption (MWh)	39.71	41.40	42.51
Average price for DRAs ($/MWh)	47.0	50.0	50.6
Network loss ratio (%)	5.27%	5.44%	5.47%

Table 4
Comparisons between three modes for 123-bus system.

	Mode 1	Mode 2	Mode 3
EUC's payoff ($)	2719.9	2746.3	2898.8
DRA payment ($)	4751.1	4832.9	4958.9
DRA consumption (MWh)	100.6	96.66	99.18
Average price for DRAs ($/MWh)	47.5	50.0	49.9
Network loss ratio (%)	6.71%	6.68%	6.78%

impact of ESS in Section 5.4. In Fig. 5, the proposed model has flattened the load curve effectively. In Fig. 6, when the electricity market price is high (e.g., 10 am to 8 pm), the transactive price signal increases and the DRA power consumption decreases. Conversely, the transactive price signal is low between midnight and 10 am, when the DRA power consumption increases. Thus, the proposed transactive DRA price can effectively reflect the underlying wholesale locational marginal prices.

In Tables 3 and 4, the EUC's payoff in mode 1 is less than that in mode 3 but higher than that in mode 2 for IEEE 33-bus system. Note that the average electricity price for DRAs in mode 1 is the lowest

Table 5
Comparisons between two methods for 33-bus test system.

	Method in [7]	Proposed method		
		L = 1	L = 2	L = 3
Number of integer variables	435	75	75	75
CPU time (s)	165.0	130.7	143.7	171.5
EUC's payoff ($)	1242.9	1252.8	1243.1	1242.3

Table 6
Comparisons between two methods for IEEE 123-bus test system.

	Method in [7]	Proposed method		
		L = 1	L = 2	L = 3
Number of integer variables	1015	175	175	175
CPU time (s)	868.0	487.2	616.0	968.8
EUC's payoff ($)	2721.3	2738.4	2725.7	2719.9

among the three modes for both IEEE 33-bus and 123-bus systems. Thus, our model can effectively alleviate the EUC's market power and guarantee the interest of DRA. Compared with mode 2, the DRA in our model consumes more power at a lower cost which shows that our model offers a more suitable retail price scheme to guarantee the interest of DRAs. For IEEE 33-bus test syetem, the network loss ratio in mode 1 is lower than that in mode 3. This indicates that peak shaving and load shifting applied in our model would lower network losses and improve the efficiency. Note that in the 123-bus system the loss ratio in mode 1 is slightly higher than that in mode 2 as DRAs in mode 1 consumes more power.

5.3. Efficiency of the proposed algorithm

We linearized complementarity constraints into disjunctive constraints through the Fortuny-Amat transformation method [7]. Numerical results for the IEEE 33-bus and the IEEE 123-bus systems are listed in Tables 5 and 6, respectively in which the objective function decreases with increasing L. Accordingly, additional segments in partitioned P^{DR} would shrink the enlarged feasible region. Thus, the proposed relaxed model achieves more accurate results. In Tables 5 and 6, when L is equal to 2, there are 0.06% and 0.2% gaps between the results presented in our method and those in [7] for 33-bus and 123-bus systems, respectively. However, the corresponding computation time is far less than that in [7]. More importantly, when L is equal to 3, our method offers more accurate results indicating that our relaxation method is tighter than that of the Fortuny-Amat transformation [7].

5.4. Sensitivity analysis

In this section, we analyze the impacts of ESS capacity and the budget of uncertainty using the IEEE 123-bus test system. We change EB from 1 to 3 MWh at 0.5 MWh steps while keeping the other parameters the same as those in mode 1 of Section 5.1. In Fig. 7(a), the EUC's payoff increases considering a higher ESS capacity which can deliver a higher level of energy when wholesale electricity prices are higher. The EUC can accordingly avoid peak prices and purchase more electricity at relatively low prices.

We change the budget from 0 to 16 at a step size of 4 while other parameters remain the same as those in mode 1 of Section 5.1. In Fig. 7(b), the EUC's payoff decreases as the budget of uncertainty increases because a larger budget allows a larger deviation in market price forecasts. Hence, the purchase cost from the wholesale market increases. Additionally, the budget choice is a tradeoff between higher payoffs and lower risks.

5.5. Accuracy of linear power flow

In order to demonstrate the accuracy of our power flow linearization, we provide the voltage magnitude difference between our results and those of the Newton-Raphson method. A comparison is also made between our method and that of [37]. In this case study, we set $\upsilon = (\overline{\mathbf{V}} - \mathbf{1})$, $\zeta = 0$ and $\overline{\mathbf{V}} = 1.05$ in the case study. Fig. 8 depicts the results where the differences obtain based on our method are much smaller than those in [37]. The results demonstrate that our linearization technique can lead to a higher accuracy for the EUC operation.

6. Conclusions and future work

In this paper, we proposed a transactive dynamic pricing scheme for DRAs that maximizes the EUC's payoff. A bi-level solution is applied in which a Nash equilibrium is calculated at the lower level for DRAs. The bilevel model is transformed into a single-level model by using the KKT conditions to represent the optimality at the lower level problem. GDP is introduced by linearizing complementarity constraints and applying the piecewise McCormick relaxation. The proposed model calculates the EUC's optimal energy procurement in the wholesale market and optimal price signal to dispatch the DR resources.

In the proposed model the lower level feasible region for each DRA depends only on its own operation constraints, while interrelations among DRAs are neglected. The coupling relationships such as spatio-temporal coupling among DRAs and the EUC will be investigated in our future efforts. In this case, the game model would be extended to the generalized Nash equilibrium and Stackelberg games in which the proposed solution method is still applicable. Besides, the method used to determine values of coefficients in the presented linearized power

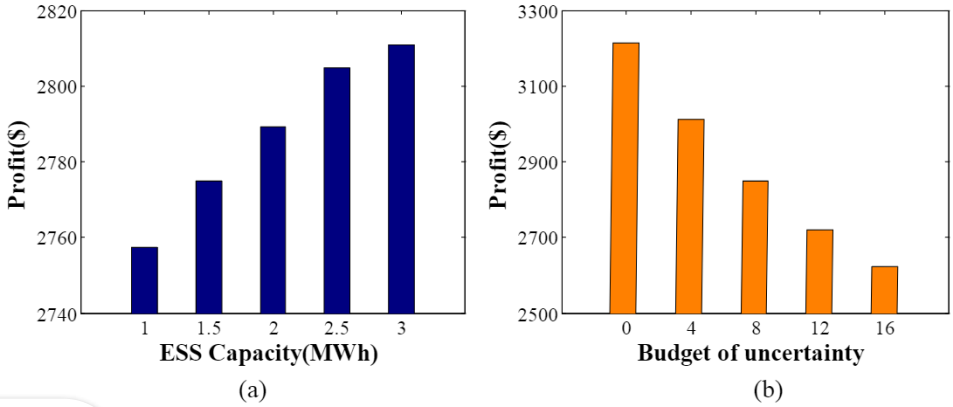

7. Sensitivity analysis: (a) Impact of ESS capacity, (b) Impact of budget of uncertainty.

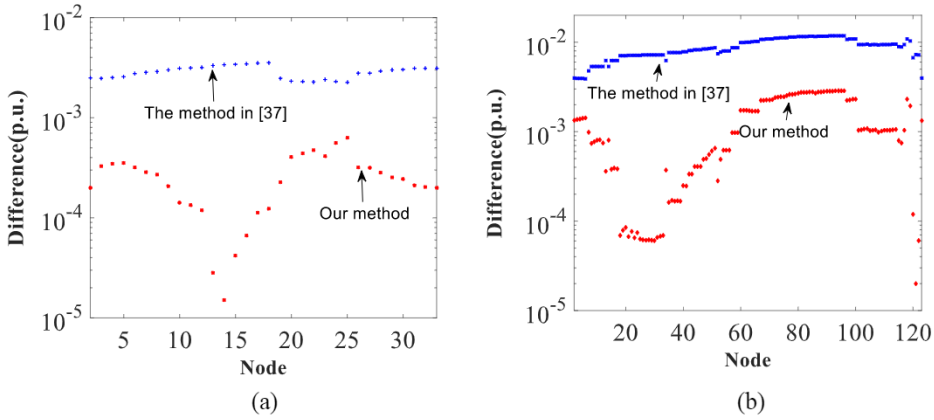

Fig. 8. Accuracy of linear power flow: (a) 33-bus test system (b) 123-bus test system.

flow model needs to be further studied. A data-driven method may be a good option to determine the optimal values of the coefficients, e.g., υ and ζ, based on field measurements in the power system

Declaration of Competing Interest

The authors declare that they have no known competing financial interests or personal relationships that could have appeared to influence the work reported in this paper.

Acknowledgment

This work is supported by National Natural Science Foundation of China (U1910216).

Appendix

A. *Determination of the uncertainty budget*

Here we present a new way to determine the uncertainty budget according to a specified confidence level. The polyhedral representation for the uncertainty is given as

$$\Omega_\lambda = \left\{ \lambda_t \mid \begin{array}{c} |\lambda_t - \widetilde{\lambda}_t| \leqslant \Delta\lambda_t \quad \forall\, t \\ \sum_{t\in\mathbf{T}} \frac{|\lambda_t - \widetilde{\lambda}_t|}{\Delta\lambda_t} \leqslant \Gamma \end{array} \right\} \tag{A1}$$

Let $\ell_t = \frac{|\lambda_t - \widetilde{\lambda}_t|}{\Delta\lambda_t}$. If $\{\lambda_t | \forall\, t \in \mathbf{T}\}$ is a sequence of independent and identically distributed random variables, then $\{\ell_t | \forall\, t \in \mathbf{T}\}$ is also a sequence of independent and identically distributed random variables. We further assume $\mathrm{E}[\ell_t] = \mu$ and $\mathrm{D}[\ell_t] = \sigma^2$. According to the Lindeberg–Lévy central limit theorem, we have

$$\lim_{T\to\infty} \sum_{t=1}^{T} \frac{\ell_t - \mu}{\sqrt{T}\sigma} \xrightarrow{d} N(0,\, 1) \tag{A2}$$

If the confidence probability for the budget constraints is set as α, we get

$$\sum_{t=1}^{T} \frac{\ell_t - \mu}{\sqrt{T}\sigma} \leqslant \Phi^{-1}(\alpha) \tag{A3}$$

Then, it attains

$$\Gamma = T\mu + \Phi^{-1}(\alpha)\sqrt{T}\sigma \tag{A4}$$

Note that although the number of time slots **T** is 24 in our work, it is assumed that the random variable $\sum_{t=1}^{T} \frac{\ell_t - \mu}{\sqrt{T}\sigma}$ approximatively converges in distribution to a normal N (0,1). When the number of time slots increases, for example to 96 (one day is divided into 96-time intervals and each interval represents 15 min), the accuracy increases accordingly. The detailed study on how the number of time slots influences the convergence of the random variable toward a normal distribution is out of scope of this paper.

Next, we present an example for deriving the expectation $\mathrm{E}[\ell_t]$ and variance $\mathrm{D}[\ell_t]$ of random variable ℓ_t. It is assumed that the wholesale electricity price λ_t is distributed normally with $\mathrm{E}[\lambda_t] = \widetilde{\lambda}_t$ and $D[\lambda_t] = (\widetilde{\lambda}_t/10)^2$. Additionally, we assume $\Delta\lambda_t = 3 * \widetilde{\lambda}_t/10$ so that the estimate interval $[\widetilde{\lambda}_t - \Delta\lambda_t, \widetilde{\lambda}_t + \Delta\lambda_t]$ can capture the true value of λ_t with a confidence level of 99.74% . On this basis, we have

$$\ell_t^o = \frac{\lambda_t - \widetilde{\lambda}_t}{\Delta\lambda_t} \xrightarrow{d} N(0,\, 1/9) \text{and } \ell_t = |\ell_t^o| \tag{A5}$$

For brevity, the subscript t is neglected hereinafter. Let $f(\ell)$ denote the probability density function with respect to random variable ℓ. We have

$$\mathrm{E}[\ell] = \int_{-\infty}^{+\infty} \ell f(\ell) d\ell = \int_{-\infty}^{+\infty} |\ell^o| \frac{3}{\sqrt{2\pi}} e^{-\frac{9(\ell^o)^2}{2}} d\ell^o = \frac{6}{\sqrt{2\pi}} \int_0^{+\infty} \ell^o e^{-\frac{9(\ell^o)^2}{2}} d\ell^o = -\frac{2}{3\sqrt{2\pi}} \int_0^{+\infty} e^{-\frac{9(\ell^o)^2}{2}} d\left(-\frac{9(\ell^o)^2}{2}\right)$$

$$= -\frac{2}{3\sqrt{2\pi}} \times (0-1) = \frac{1}{3}\sqrt{\frac{2}{\pi}} \tag{A6}$$

$$\mathrm{D}[\ell] = \mathrm{E}[\ell^2] - \mathrm{E}[\ell]^2 = \mathrm{E}[(\ell^o)^2] - \mathrm{E}[\ell]^2 = \mathrm{D}[\ell^o] + \mathrm{E}[\ell^o]^2 - \mathrm{E}[\ell]^2 = \frac{1}{9}\left(1 - \frac{2}{\pi}\right) \tag{A7}$$

When the confidence probability for the budget constraints is set as 99.99%, the lower limit for the budget is 7.17.

B. The linearized power flow equations

In order to speed up solution process, a new formulation of the linearized AC power flow is devised. At first, the bus injection model is formulated as:

$$\mathbf{S} = diag(\mathbf{V})\mathbf{I}^* = diag(\mathbf{V})(\overline{\mathbf{Y}}^* V_0 + \mathbf{Y}_N^* \mathbf{V}^*) \tag{B1}$$

$$\begin{bmatrix} I_0 \\ \mathbf{I} \end{bmatrix} = \mathbf{Y}\begin{bmatrix} V_0 \\ \mathbf{V} \end{bmatrix} = \begin{bmatrix} y_0 & \overline{\mathbf{Y}}' \\ \overline{\mathbf{Y}} & \mathbf{Y}_N \end{bmatrix}\begin{bmatrix} V_0 \\ \mathbf{V} \end{bmatrix} \tag{B2}$$

where the admittance matrix $\mathbf{Y}$ is partitioned into a 1×1 matrix y_0, a $(N-1) \times 1$ column vector $\overline{\mathbf{Y}}$, a $(N-1) \times (N-1)$ square matrix $\mathbf{Y}_N$. We assume bus 0 is the slack bus. For a given vector $\mathbf{x}$, $diag(\mathbf{x})$ denotes a diagonal matrix whose diagonal elements are composed of $\mathbf{x}$.

Next, a linear approximation of AC power flow in rectangular coordinates is given. According to (B2),

$$\mathbf{I} = \overline{\mathbf{Y}} V_0 + \mathbf{Y}_N \mathbf{V} \tag{B3}$$

Let $\overline{\mathbf{V}}$ denote the vector of upper limit of the nodal voltage magnitude. If $\mathbf{V} = \overline{\mathbf{V}} + \Delta\mathbf{V}$, expanding (B1), we get:

$$\mathbf{S} - \Xi = \Theta\Delta\mathbf{V} + \Pi\Delta\mathbf{V}^* + diag(\Delta\mathbf{V})(\mathbf{Y}_N^*\Delta\mathbf{V}^*) \tag{B4}$$

where

$$\begin{cases} \Xi = diag(\overline{\mathbf{V}})(\overline{\mathbf{Y}}^* V_0^*) + diag(\overline{\mathbf{V}})(\mathbf{Y}_N^*\overline{\mathbf{V}}^*) \\ \Pi = diag(\overline{\mathbf{V}})\mathbf{Y}_N^* \\ \Theta = diag(\overline{\mathbf{Y}}^* V_0^* + \mathbf{Y}_N^*\overline{\mathbf{V}}^*) \end{cases} \tag{B5}$$

Note that all the nonlinear terms exist in $diag(\Delta\mathbf{V})(\mathbf{Y}_N^*\Delta\mathbf{V}^*)$. For brevity, let $f(\Delta\mathbf{V}, \Delta\mathbf{V}^*)$ represent $diag(\Delta\mathbf{V})(\mathbf{Y}_N^*\Delta\mathbf{V}^*)$. Obviously, $f(\Delta\mathbf{V}, \Delta\mathbf{V}^*)$ is continuously differentiable with respect to the real and imaginary parts of $\Delta\mathbf{V}$. According to the work in [39], the following formulation is used to linearize the function f.

$$f(\Delta\mathbf{V}, \Delta\mathbf{V}^*) \approx \mathbf{J}|_{\substack{Re(\Delta\mathbf{V})=\upsilon \\ Im(\Delta\mathbf{V})=\zeta}} \begin{bmatrix} \mathrm{Re}(\Delta\mathbf{V}) \\ \mathrm{Im}(\Delta\mathbf{V}) \end{bmatrix} \tag{B6}$$

where $\mathbf{J} = [\partial f/\partial(Re(\Delta\mathbf{V}))\ \ \partial f/\partial(\mathrm{Im}(\Delta\mathbf{V}))]$ which is a complex Jacobian matrix. Here we abuse the concept of mean value in the *mean value theorem*. υ and ζ can be seen as the mean values of the real and imaginary parts of $\Delta\mathbf{V}$, respectively. Thus, it yields:

$$\begin{bmatrix} \mathbf{P} - \mathrm{Re}(\Xi) \\ \mathbf{Q} - Im(\Xi) \end{bmatrix} = \left(\begin{bmatrix} \mathrm{Re}(\Theta + \Pi) & \mathrm{Im}(\Pi - \Theta) \\ \mathrm{Im}(\Theta + \Pi) & \mathrm{Re}(\Theta - \Pi) \end{bmatrix} + \begin{bmatrix} \mathrm{Re}(\mathbf{J}) \\ \mathrm{Im}(\mathbf{J}) \end{bmatrix}_{\substack{Re(\Delta\mathbf{V})=\upsilon \\ Im(\Delta\mathbf{V})=\zeta}} \right) \begin{bmatrix} \mathrm{Re}(\Delta\mathbf{V}) \\ \mathrm{Im}(\Delta\mathbf{V}) \end{bmatrix} \tag{B7}$$

Obviously, the values of υ and ζ play a pivotal role in the accuracy of the linearized model above. In a non-stressed system, bus voltage magnitudes are usually close to 1 p.u. and phase angle differences are nearly equal to zero. For simplicity, the flat voltage solution is applicable where $\upsilon = (\overline{\mathbf{V}} - \mathbf{1})$ and $\zeta = 0$. Note that it is assumed there exist only PQ buses and slack bus in a distribution system. As for the systems including PV buses, the similar equation for the nodal voltage magnitude can be obtained. Besides, the same approach can be adopted to derive a linearized model for unbalanced multi-phase grid in a similar manner and we do not repeat it again.

In addition, through some reasonable assumptions, (B4) can be transformed into DC power flow formulations. First, neglecting the nonlinear terms in (B4) yields

$$\mathbf{S} - \Xi = \Theta\Delta\mathbf{V} + \Pi\Delta\mathbf{V}^* \tag{B8}$$

Specifically, the real part of (B8) can be written as

$$\mathbf{P} - \mathrm{Re}(\Xi) = \mathrm{Re}(\Theta\Delta\mathbf{V}) + \mathrm{Re}(\Pi\Delta\mathbf{V}^*) \tag{B9}$$

By assuming zero shunt admittances and defining $\overline{\mathbf{V}} = \mathbf{1}$, then $\mathrm{Re}(\Xi) = \mathbf{0}$ and $\mathrm{Re}(\Theta\Delta\mathbf{V}) = 0$.

On this basis, (B9) can be written as $\mathbf{P} = \mathrm{Re}(\Pi\Delta\mathbf{V}^*) = \mathrm{Re}(\mathbf{Y}_N)\,\mathrm{Re}(\Delta\mathbf{V}) - \mathrm{Im}(\mathbf{Y}_N)\mathrm{Im}(\Delta\mathbf{V})$. If lines are purely inductive, i.e., $\mathrm{Re}(\mathbf{Y}_N) = 0$, then

$$\mathbf{P} = -\mathrm{Im}(\mathbf{Y}_N)\mathrm{Im}(\Delta\mathbf{V}) \tag{B10}$$

Since the angle difference between the two terminals of a transmission line is usually small and $\theta \approx \mathrm{Im}(\Delta\mathbf{V})$, then when the angle is represented in radians, the following equation can be attained:

$$\mathbf{P} = -\mathrm{Im}(\mathbf{Y}_N)\theta \tag{B11}$$

(B11) is actually the DC power flow model. As the proposed model can address nonlinear terms in (B4) without the above simplifications required, and hence can attain more accurate solutions.

C. Proof of the theorem

Here, we present a detailed proof based on the method proposed in [38]. The utility function in our model is linearized by a piecewise-linear function. As a large number of demand response resources are aggregated, we approximately assume the power of each DRA $\mathbf{P}_{d,t}^{DR}$ is a continuous variable.

For brevity, we define $P_{\mathbf{D},t}^{DR} = \sum_{d\in\mathbf{D}} P_{d,t}^{DR}$ and $\mathbf{P}_{\mathbf{D}}^{DR} = \sum_{d\in\mathbf{D}} \mathbf{P}_{\mathbf{T},d}^{DR}$. We define $\sigma(\mathbf{x}) = \sum_{i}^{n} \varphi_i(\mathbf{x})$ and the pseudo gradient of $\sigma(\mathbf{x})$ can be defined as follows:

$$g(\mathbf{x}) = [\nabla_1\varphi_1(x), ...,\nabla_n\varphi_n(x)]' \tag{C1}$$

Definition: $\sigma(\mathbf{x})$ is diagonally strictly concave for $\mathbf{x}$ if for every $\mathbf{x}^1$, $\mathbf{x}^0$, we have

$$(\mathbf{x}^1 - \mathbf{x}^0)'g(\mathbf{x}^0) + (\mathbf{x}^0 - \mathbf{x}^1)'g(\mathbf{x}^1) > 0 \tag{C2}$$

where x' denotes the transpose of x.

Next, we show $\sum_{d\in\mathbf{D}} f_d^{DR}(\mathbf{P}_1^{DR}, ...,\mathbf{P}_D^{DR})$ is diagonally strictly concave. According to (C1), we get

$$g(\mathbf{P}_{\mathbf{T},1}^{DR}, ...,\mathbf{P}_{\mathbf{T},D}^{DR}, U_{\mathbf{T},1}^{DR}, ...,U_{\mathbf{T},D}^{DR}) = [\nabla_1 f_1^{DR}, ...,\nabla_D f_D^{DR}]' \tag{C3}$$

where $[\nabla_1 f_1^{DR}, ...,\nabla_D f_D^{DR}]' = [-\varphi(\mathbf{P}_{\mathbf{D}}^{DR} + \mathbf{P}_{\mathbf{T},1}^{DR} + \mathbf{P}_{\mathbf{N}}^{L}) + \vartheta, ...,-\varphi(\mathbf{P}_{\mathbf{D}}^{DR} + \mathbf{P}_{\mathbf{T},D}^{DR} + \mathbf{P}_{\mathbf{N}}^{L}) + \vartheta, \underbrace{1, ...,1}_{D}]'$

Define:

$$\mathbf{x}^1 = [\mathbf{P}_{\mathbf{T},1}^{DR(1)}, ...,\mathbf{P}_{\mathbf{T},D}^{DR(1)}, U_1^{DR(1)}, ...,U_D^{DR(1)}] \tag{C4}$$

$$\mathbf{x}^0 = [\mathbf{P}_{\mathbf{T},1}^{DR(0)}, ...,\mathbf{P}_{\mathbf{T},D}^{DR(0)}, U_1^{DR(0)}, ...,U_D^{DR(0)}] \tag{C5}$$

Substituting (C4) and (C5) into (C2), as $\varphi \geqslant 0$ and $\mathbf{x}^1 \neq \mathbf{x}^0$, we have,

$$\varphi \|\mathbf{P}_{\mathbf{D}}^{DR(1)} - \mathbf{P}_{\mathbf{D}}^{DR(0)}\|_2^2 + \varphi \sum_{d\in\mathbf{D}} \|\mathbf{P}_{\mathbf{T},d}^{DR(1)} - \mathbf{P}_{\mathbf{T},d}^{DR(0)}\|_2^2 > 0 \tag{C6}$$

Thus, $\sigma(\mathbf{P}_{\mathbf{T},1}^{DR}, ...,\mathbf{P}_{\mathbf{T},D}^{DR})$ is diagonally strictly concave. In addition, $f_d^{DR}(\mathbf{P}_{\mathbf{T},d}^{DR}, \mathbf{P}_{\mathbf{T},-d}^{DR})$ is a concave function (In our model it is a concave quadratic function) and the allowed strategies are limited by the requirement that the decision variables (e.g., $\mathbf{P}_{\mathbf{T},d}^{DR}$) is selected from a convex and closed set (In our model it is a closed polyhedral set as represented by $\mathbf{X}_d^{DR}$). According to Theorems 1 and 2 in [38], a Nash equilibrium always exists and is unique.

D. Determination of the M in disjunctive constraints

Here we show how to determine the lower limit of M in (35). The Lagrangian multiplier α_d^4 is the sensitivity of the objective function (13) of DRA with respect to the right hand term $\sum_{t\in\mathbf{T}} P_{d,t}^{DR}$. Suppose that E_d^{DR} increases to $E_d^{DR} + \Delta E_d^{DR}$, the optimal value of objective function of DRA d is also changed accordingly. First, let us investigate the change in the cost term. The maximal incremental cost may happen at the highest retail price period. Thus, the incremental cost ΔC_d respects the following inequality:

$$\begin{aligned}\Delta C_d &\leqslant \max_{t\in\mathbf{T}}\{\Delta E_d^{DR} * \gamma_t^{DR}\} \\ &= \max_{t\in\mathbf{T}}\{\Delta E_d^{DR} * \varphi(P_{\mathbf{D},t}^{DR} + P_{\mathbf{N},t}^{L}) + \Delta E_d^{DR} * (\vartheta_{base} + \widetilde{\vartheta} * \psi_t)\} \\ &\leqslant \max_{t\in\mathbf{T}}\left\{\Delta E_d^{DR} * \varphi\left(\sum_{d\in\mathbf{D}} \overline{P}_{d,t}^{DR} + P_{\mathbf{N},t}^{L}\right) + \Delta E_d^{DR} * (\vartheta_{base} + \widetilde{\vartheta} * |\psi|)\right\}\end{aligned} \tag{D1}$$

The maximal change in the utility function is described as

$$\Delta U_d \leqslant \max_{k\in\{1,...,K\}}\{\Delta E_d^{DR} * a_{d,k,t}\} \tag{D2}$$

Let ΔQ_d denote the change in the objective function. Both C_d and U_d increase monotonically with respect to $\sum_{t\in\mathbf{T}} P_{d,t}^{DR}$. Therefore, $\Delta C_d \geqslant 0$ and $\Delta U_d \geqslant 0$. We have

$$\Delta Q_d = \Delta U_d - \Delta C_d \leqslant \Delta C_d + \Delta U_d \tag{D3}$$

As a result, we get

$$\begin{aligned}\alpha_d^4 &\leqslant |\Delta Q_d/\Delta E_d^{DR}| \leqslant |\Delta C_d + \Delta U_d|/\Delta E_d^{DR} \\ &\leqslant \max_{t\in\mathbf{T}}\left\{\varphi\left(\sum_{d\in\mathbf{D}} \overline{P}_{d,t}^{DR} + P_{\mathbf{N},t}^{L}\right) + (\vartheta_{base} + \widetilde{\vartheta} * |\psi|)\right\} + \max_{k\in\{1,...,K\}}\{a_{d,k,t}\} = M\end{aligned} \tag{D4}$$

We assume DRA has the same utility function for every time interval. If not, we enumerate all time intervals and choose the largest one to substitute into (D4).

The above is seen as a general method to determine an appropriate value of M. Besides, in our model as we can determine the sign of ΔC_d and ΔU_d in advance, we derive a tighter lower limit on M. As ΔE_d^{DR} increases to $E_d^{DR} + \Delta E_d^{DR}$, we have $\Delta Q_d \leqslant 0$. Thus, it is only necessary to calculate the minimal value of ΔQ_d. Thus,

If $\min_{t\in\mathbf{T}}\{\Delta E_d^{DR} * a_{d,k,t}\} \leqslant \max_{t\in\mathbf{T}}\{\Delta E_d^{DR} * \varphi(\sum_{d\in\mathbf{D}} \overline{P}_{d,t}^{DR} + P_{\mathbf{N},t}^{L}) + \Delta E_d^{DR} * (\vartheta_{base} + \widetilde{\vartheta} * |\psi|)\}$

$$\alpha_d^4 \leqslant |\Delta Q_d/\Delta E_d^{DR}| \leqslant \max_{t\in \mathbf{T}}\left\{\varphi\left(\sum\nolimits_{d\in \mathbf{D}} \overline{P}_{d,t}^{DR} + P_{\mathrm{N},t}^{L}\right) + (\vartheta_{base} + \widetilde{\vartheta} * |\psi|)\right\} - \min_{k\in\{1,\ldots,K\}}\{a_{d,k,t}\} = M \tag{D5}$$

Otherwise, according to $\Delta Q_d \leqslant 0$ and $\Delta Q_d = \Delta U_d - \Delta C_d \geqslant 0$, we have

$$\Delta Q_d = 0 \text{and } 0 \leqslant \alpha_d^4 \leqslant |\Delta Q_d/\Delta E_d^{DR}| = 0 \tag{D6}$$

In this case, $M = 0$. This is reasonable because ΔQ_d equal to zero implies that the inequality (35) is not binding and thus the corresponding Lagrangian multiplier is zero. In our model, M is set at 120.

Appendix A. Supplementary material

Supplementary data to this article can be found online at https://doi.org/10.1016/j.ijepes.2019.105764.

References

[1] Cappers P. Time-of-use as a default rate for residential customers: Issues and insights. Lawrence Berkeley Nat. Lab., Berkeley, CA, USA, LBNL-1005704, Jun. 2016.
[2] Li Z, Shahidehpour M, Aminifar F. Networked microgrids for enhancing the power system resilience. Proc IEEE 2017;105(7):1289–310.
[3] Elghitani F, Zhang W. Aggregating a large number of residential appliances for demand response applications. IEEE Trans Smart Grid 2018;9(5):5092–100.
[4] Wei W, Liu F, Mei XW. Energy pricing and dispatch for smart grid retailers under demand response and market price uncertainty. IEEE Trans Smart Grid 2015;6(3):1364–74.
[5] Mohsenian-Rad A, Wong V, Jatskevich J. Autonomous demand-side management based on game-theoretic energy consumption scheduling for the future smart grid. IEEE Trans Smart Grid 2010;3(3):320–31.
[6] Haghighat H, Kennedy S. A bi-level approach to operational decision making of a distribution company in competitive environments. IEEE Trans Power Syst 2012;27(4):1797–807.
[7] Nguyen DT, Nguyen HT, Le LB. Dynamic pricing design for demand response integration in power distribution networks. IEEE Trans Power Syst 2016;31(5):3457–72.
[8] Zugno M, Morales JM, Pinson P, Madsen H. A bilevel model for electricity retailers' participation in a demand response market environment. Energy Econ 2013;36:182–97.
[9] Vaya MG, Andersson G. Optimal bidding strategy of a plug-in electric vehicle aggregator in day-ahead electricity markets under uncertainty. IEEE Trans Power Syst 2015;30(5):2375–85.
[10] Ruiz C, Conejo AJ. Pool strategy of a producer with endogenous formation of locational marginal prices. IEEE Trans Power Syst 2009;24(4):1855–66.
[11] Li Z, Shahidehpour M, et al. Bilevel model for analyzing coordinated cyber-physical attacks on power systems. IEEE Trans Smart Grid 2016;7(5):2260–72.
[12] Momber I, Worgin S, Roman TGS. Retail pricing: a bilevel program for PEV aggregator decision using indirect load control. IEEE Trans Power Syst 2016;31(1):464–73.
[13] Arroyo J. Bilevel programming applied to power system vulnerability analysis under multiple contingencies. IET Gener Transm Distrib 2010;4(2):178–90.
[14] Keyffer S, Munson T. Solving multi-leader-follower games. Optimiz Meth Softw 2010;25:601–23.
[15] Anstreicher KM. Semidefinite programming versus the reformulation-linearization technique for nonconvex quadratically constrained quadratic programming. J Global Optim 2009;43:471–84.
[16] Castro P. Tightening piecewise McCormick relaxations for bilinear problems. Comput Chem Eng 2005;72:300–11.
[17] Lee S, Grossmann IE. New algorithms for nonlinear generalized disjunctive programming. Comput Chem Eng 2000;25:2125–41.
[18] The GridWise architecture council. GridWise transactive energy framework. Tech. Rep. PNNL-22946, Jan. 2015.
[19] Hao H, Corbin C, Kalsi K, et al. Transactive control of commercial buildings for demand response. IEEE Trans Power Syst 2017;32(1):774–83.
[20] Hu J, Yang G, Bindner H, et al. Application of network-constrained transactive control of electric vehicle charging for secure grid operation. IEEE Trans Sustain Energy 2017;8(2):505–15.
[21] Nunna HK, Srinivasan D. Multiagent-based transactive energy framework for distribution systems with smart microgrids. IEEE Trans Ind Informat 2017;13(5):2241–50.
[22] Li S, Zhang W, Lian J, Kalsi K. Market-based coordination of thermostatically controlled loads-Part I: A mechanism design formulation. IEEE Trans Power Syst 2016;31(2):1170–8.
[23] Lee J, Guo JY, Choi JK, et al. Distributed energy trading in microgrids: a game-theoretic model and its equilibrium analysis. IEEE Trans Ind Electron 2015;62(6):3524–33.
[24] Atzeni I, Ordonez L, Scutari G, Palomar D, Fonollosa J. Demand-side Management via distributed energy generation and storage optimization. IEEE Trans Smart Grid 2013;4(2):866–76.
[25] Baharlouei Z, Narimani H, Hashemi M. On the convergence properties of autonomous demand side algorithms. IEEE Trans Smart Grid 2017;9(6):6713–20.
[26] Rahimiyan M, Baringo L, Conejo AJ. Energy management of a cluster of interconnected price-responsive demands. IEEE Trans Power Syst 2014;29(2):645–55.
[27] Fahrioglu M, Alvarado F. Using utility information to calibrate customer demand management behavior models. IEEE Trans Power Syst 2001;16(2):317–22.
[28] Lu T, Wang Z, Wang J, Ai Q, Wang C. A data-driven stackelberg market strategy for demand response-enabled distribution systems. IEEE Trans. Smart Grid 2019;10(3):2345–57.
[29] Bertsimas D, Sim M. The price of robustness. Oper Res 2004;52(1):35–53.
[30] Alipour M, Zare K, Zareipour H, Seyedi H. Heading strategies for heat and electricity consumers in the presence of real-time demand response programs. IEEE Trans Sustainable Energy 2019;10(3):1262–70.
[31] Bertsimas D. Robust discrete optimization and network flows. Math Program 2003;98(1–3):49–71.
[32] Chen Z, Wu L, Fu Y. Real-time price-based demand response management for residential appliances via stochastic optimization and robust optimization. IEEE Trans Sustainable Energy 2012;3(4):1822–31.
[33] Samadi P, Mohsenian-Rad A, Schober R, Wong V, Jatskevich J. Optimal real-time pricing algorithm based on utility maximization for smart grid. In Proc. IEEE Int. Conf. Smart Grid Commun., Gaithersburg, MD, USA; 2010. p. 415–20.
[34] Feng C, Li Z, Shahidehpour M, et al. Decentralized short-term voltage control in active power distribution systems. IEEE Trans Smart Grid 2018;9(5):4566–76.
[35] PJM Data [Online]. Available: http://www.pjm.com/markets-and-operations/energy.aspx. Accessed on: July 22, 2018.
[36] System data [Online]. Available: http://motor.ece.iit.edu/data/DPS.xls.
[37] Dhople S, Guggilam S. Linear approximations to AC power flow in rectangular coordinates. In: Proc. of 53rd Annual Allerton Conf. on Commun., Control, and Comp., Monticello, IL, Oct. 2015. p. 1–5.
[38] Rosen JB. Existence and uniqueness of equilibrium points for concave n-person games. Econometrica 1965;33:347–51.
[39] Bolognani S, Dorfler F. Fast power system analysis via implicit linearization of the power flow manifold. In: Proc. of 53rd Annual Allerton Conference, Allerton House, UIUC, Il. Oct. 2015. p. 1–7.